KI REPORTS
KIReports.org
TRANSLATIONAL RESEARCH

Impact of Induction Therapy on Circulating T Follicular Helper Cells and Subsequent Donor-Specific Antibody Formation After Kidney Transplant

Camila Macedo[1,2], Kevin Hadi[1,2], John Walters[1,2], Beth Elinoff[1,2], Marilyn Marrari[1,3], Adriana Zeevi[1,3,4], Bala Ramaswami[1,2], Geetha Chalasani[1,4,5], Douglas Landsittel[1,6], Adele Shields[7], Rita Alloway[8], Fadi G. Lakkis[1,4,5], E. Steve Woodle[7] and Diana Metes[1,2,4]

[1]Thomas E. Starzl Transplantation Institute, University of Pittsburgh Medical Center, Pittsburgh, Pennsylvania, USA; [2]Department of Surgery, University of Pittsburgh, Pittsburgh, Pennsylvania, USA; [3]Department of Pathology, University of Pittsburgh, Pittsburgh, Pennsylvania, USA; [4]Department of Immunology, University of Pittsburgh, Pittsburgh, Pennsylvania, USA; [5]Department of Medicine, University of Pittsburgh, Pittsburgh, Pennsylvania, USA; [6]Department of Biomedical Informatics, University of Pittsburgh, Pittsburgh, Pennsylvania, USA; [7]Division of Transplantation, University of Cincinnati, Cincinnati, Ohio, USA; and [8]Division of Nephrology, University of Cincinnati, Cincinnati, Ohio, USA

Introduction: The cellular events that contribute to generation of donor-specific anti-HLA antibodies (DSA) post-kidney transplantation (KTx) are not well understood. Characterization of such mechanisms could allow tailoring of immunosuppression to benefit sensitized patients.

Methods: We prospectively monitored circulating T follicular helper (cT_{FH}) cells in KTx recipients who received T-cell depleting (thymoglobulin, $n = 54$) or T-cell nondepleting (basiliximab, $n = 20$) induction therapy from pre-KTx to 1 year post-KTx and assessed their phenotypic changes due to induction and DSA occurrence, in addition to healthy controls ($n = 13$), for a total of 307 blood samples.

Results: Before KTx, patients displayed comparable levels of resting, central memory cT_{FH} cells with similar polarization to those of healthy controls. Unlike basiliximab induction, thymoglobulin induction significantly depleted cT_{FH} cells, triggered lymphopenia-induced proliferation that skewed cT_{FH} cells toward increased Th1 polarization, effector memory, and elevated programmed cell death protein 1 $(PD\text{-}1)^{int/hi}$ expression, resembling activated phenotypes. Regardless of induction, patients who developed DSA post-KTx, harbored pre-KTx donor-reactive memory interleukin $(IL)\text{-}21^{+}$ cT_{FH} cells and showed higher % cT_{FH} and lower % of T regulatory (T_{REG}) cells post-KTx resulting in elevated cT_{FH}:T_{REG} ratio at DSA occurrence.

Conclusion: Induction therapy distinctly shapes cT_{FH} cell phenotype post-KTx. Monitoring cT_{FH} cells before and after KTx may help detect those patients prone to DSA generation post-KTx.

Kidney Int Rep (2019) **4,** 455–469; https://doi.org/10.1016/j.ekir.2018.11.020
KEYWORDS: donor-specific anti-HLA antibody; kidney transplantation; T follicular helper cells; thymoglobulin

One biomarker that has a strong association with poor long-term kidney allograft outcomes is the presence of DSAs in transplant (Tx) recipients.[1–3] Recent literature has established that DSA contributes to a wide range of allograft pathology that includes symptomatic acute antibody-mediated rejection, subclinical antibody-mediated rejection, or asymptomatic DSA without graft injury.[4–7] Moreover, approximately one-half of kidney Tx (KTx) patients with asymptomatic DSA have significantly lower long-term allograft survival, driven by chronic subclinical antibody-mediated rejection.[6] Therefore, there is a need to understand what mechanistic events are involved in DSA generation, how induction therapy and immunosuppression affect such mechanisms, and how to target them to improve long-term outcomes. Novel noninvasive immunologic monitoring implemented alongside available platforms would enhance detection of pre-KTx donor-specific humoral memory in the absence of detectable sensitization,

Correspondence: Diana Metes, Thomas E. Starzl Transplantation Institute and Departments of Surgery and Immunology, University of Pittsburgh, E 1549 Thomas E. Starzl Biomedical Science Tower, 200 Lothrop Street, Pittsburgh, Pennsylvania 15213, USA. E-mail: metesdm@upmc.edu

Received 24 September 2018; revised 24 October 2018; accepted 26 November 2018; published online 7 December 2018

especially for those patients considered low-risk (DSA^-), but who are presensitized against their donor. This would improve patient risk stratification and post-Tx monitoring for implementation of personalized induction and immunosuppression maintenance.

DSAs are isotype-switched IgG antibodies (Abs) directed against HLA molecules that depend on T-cell help for their generation. T follicular helper (T_{FH}) cells, a subset of memory ($CD45RO^+$) $CXCR5^+CD4^+$ T cells, participate in the germinal center formation in secondary lymphoid organs, where they provide critical cognate antigenic help to B lymphocytes inducing their differentiation into memory B cells, short-lived plasmablasts, and/or long-lived plasma cells that secrete high-affinity, isotype-switched IgG responses.[8–10]

Human peripheral blood $CXCR5^+CD4^+$ T cells, also called circulating (c)T_{FH} cells, are considered the counterparts of germinal center–T_{FH} cells and represent approximately 20% of peripheral blood memory $CD4^+$ T cells.[11–13] $_cT_{FH}$ cells are functionally heterogeneous and, based on their distinct chemokine receptor coexpression and ability to produce cytokines, comprise Th1-cT_{FH} ($CXCR3^+$), Th2- and Th17-cT_{FH} ($CXCR3^-$) subsets. These subsets convey critically different somatic hypermutation instructions to antigen (Ag)-specific B cells that distinctly shape antibody responses.[12,14] In addition, differential coexpression of PD-1 and CD62L further identifies cT_{FH} cell activation status as activated ($PD\text{-}1^{hi}CD62L^{lo}$), partially activated ($PD\text{-}1^{int}CD62L^{int}$), and quiescent ($PD\text{-}1^{lo}CD62L^{hi}$).[11] Monitoring cT_{FH} cell subset distribution and phenotypes in human blood has been shown to be a good surrogate to identify T_{FH} cell activation (i.e., Ab responses) in healthy humans after vaccination or in patients with chronic Ab-mediated diseases.[13,15,16]

Approximately 60% of solid organ transplant recipients in the United States receive thymoglobulin, a T-cell depleting agent, as induction therapy, whereas approximately 20% receive the non–T-cell depleting anti-IL-2Rα blocker basiliximab. Thymoglobulin induction was shown to trigger significant and protracted depletion of total $CD4^+$ T lymphocytes.[17–19] Lymphopenia-induced proliferation (LIP) after depletion initiates repopulation of $CD4^+$ T cells with a phenotype skewed toward effector memory pool and a significant decrease in the naïve pool.[20] Conversely, literature reports that the frequency and memory differentiation of $CD4^+$ T cells post-basiliximab induction remains unchanged.[19] However, the effect of induction therapy on cT_{FH} cell levels and phenotype post-KTx, and how these impact changes in cT_{FH} cells during DSA responses have not been thoroughly investigated in the field of organ transplantation.[21–24] Our goal here was to elucidate in a longitudinal and cross-sectional manner the impact of this T-cell depleting agent thymoglobulin on the levels and phenotype of cT_{FH} cells and correlate those with the development of DSA post-KTx. Basiliximab induction was used as a control group.

METHODS

Patients and Immunosuppression

A cohort of consecutive 56 first-time living donor ABO-compatible KTx recipients (thymoglobulin-induced $n = 34$ and basiliximab-induced $n = 22$) was recruited between October 2011 and September 2014 following informed consent at Christ Hospital and University of Cincinnati (TCH no. 11-44; IRB no. 11-06-09-05EE) and enrolled into a prospective 12-month study (Figure 1). By the end of study follow-up, 31 thymoglobulin- and 20 basiliximab-induced patients remained eligible for our immunologic analyses. There were no significant differences in gender, number of HLA mismatches, degree of presensitization (by percent reactive Ag, flow cytometry cross-match, DSA, history of pregnancies and transfusions) and maintenance immunosuppression between cohorts (Table 1). Etiologies of end-stage renal disease (ESRD), including autoimmune and inflammatory kidney disease are found in Supplementary Table S1. In addition, 13 gender- and age-matched healthy control (HC) volunteers were recruited on informed consent at the University of Pittsburgh (IRB no. 0608014) and used as controls (Table 1).

An independent cross-sectional cohort of thymoglobulin-induced patients ($n = 23$) was recruited from the University of Pittsburgh Medical Center (UPMC) (IRB no. 12030552) and included in the study as part of a validation group (Figure 1, Supplementary Tables S2 and S3).

Whole-Blood Collection

Blood samples were obtained prospectively from pre-Tx to 30, 90, 180, 270, and 360 days post-KTx from the Cincinnati cohort (Figure 1c) and cross-sectional from the UPMC cohort (Figure 1d). One milliliter of whole blood was used for flow cytometry, whereas the remainder to isolate plasma and peripheral blood mononuclear cells (PBMCs) by Ficoll-Hypaque (GE Healthcare, Uppsala, Sweden) and subsequently banked. Overall, a total of 307 samples were collected and analyzed by flow cytometry for cT_{FH} characterization and by single-bead Luminex for anti-HLA antibody detection.

DSA Definition

We classified patients as stable (no DSA, no rejection or infection throughout follow-up) or DSA^+. DSA^+ patients were defined as patients who became positive for DSA post-KTx (≥1000-mean fluorescence intensity [MFI]). According to this definition, 19 patients (Cincinnati cohort $n = 12$ and UPMC cohort $n = 7$) were classified as DSA^+ (Table 2 and Supplementary

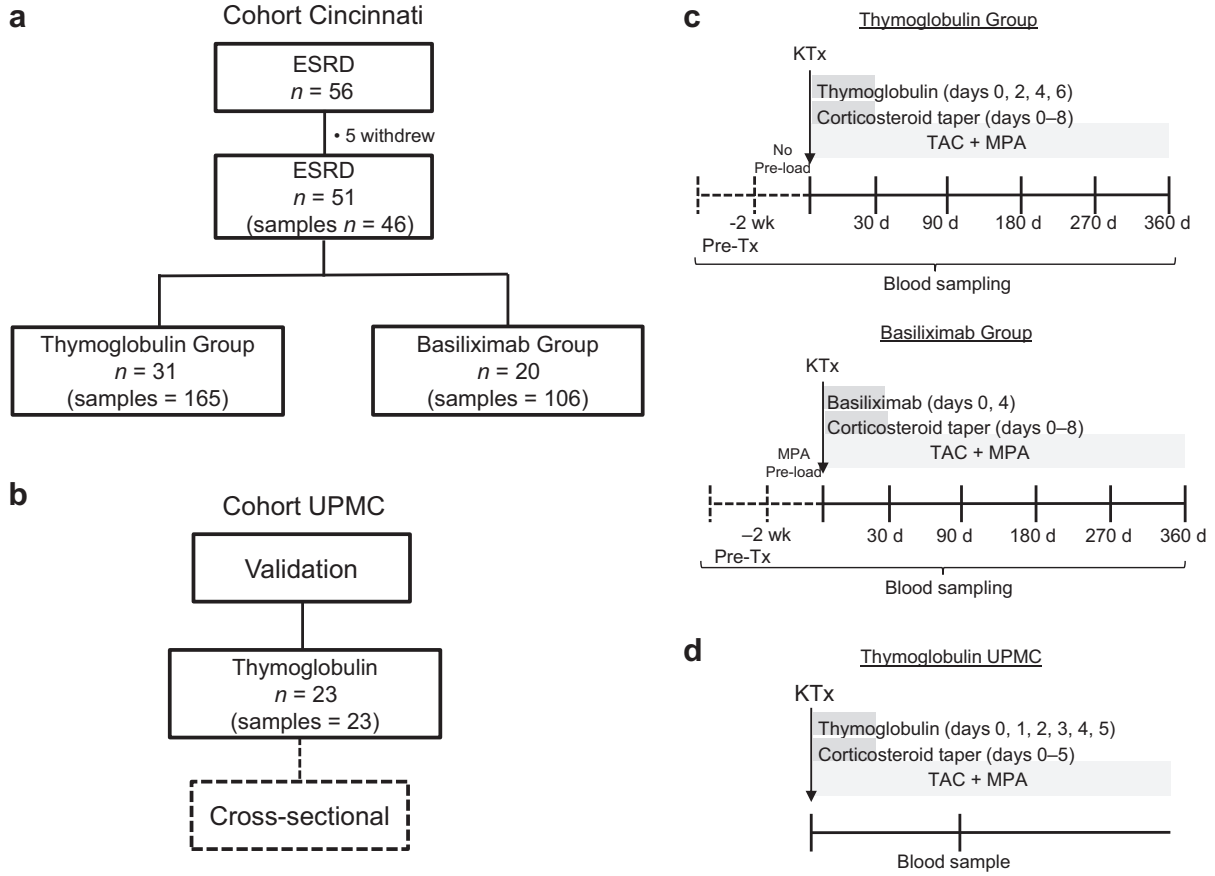

Figure 1. Flowchart representation of cohort of patients, their induction therapy, and prospective blood sampling. (a) Schematic representation of the study design and the number of participating patients and samples tested from the Cincinnati cohort and (b) from the University of Pittsburgh Medical Center (UPMC) cohort. (c) Diagram of induction therapy/immunosuppression regimen. T-cell–depleted patients received thymoglobulin at 1.5 mg/kg per dose i.v. × 4 doses given on postoperative day (POD) 0, 2, 4, and 6 plus solumedrol perioperative as 10 mg/kg i.v. (maximum 500 mg), followed by taper discontinued by POD 8. Patients in the T-cell–nondepleted group received mycophenolic acid (MPA) preload 2 weeks before kidney transplantation (KTx) (720 mg p.o. 2x daily) followed by basiliximab induction at 20 mg i.v. × 2 doses given on POD 0 and 4 plus a steroid taper as described previously. Maintenance immunosuppression consisted of Tacrolimus (TAC) 0.05 mg/kg orally twice daily (target trough level at POD 0–89 = 8–15 ng/ml and POD > 90 = 5–10 ng/ml) and MPA 720 mg orally twice daily starting on the day of transplantation for both cohorts. Blood samples were prospectively collected up to 1 year post-KTx as indicated. The pre-Tx sample was always collected before induction and/or MPA preload. (d) Diagram of induction therapy/immunosuppression regimen from the validation UPMC cohort. Patients received thymoglobulin at 1.5 mg/kg per dose i.v. × 5 doses given on POD 0–5 plus premedication with acetaminophen 650 mg, diphenhydramine 25 mg, and daily methylprednisolone dose-tapering 1 hour 30 minutes before infusion for 5 days. Maintenance immunosuppression consisted of TAC 0.05–0.1 mg/kg orally twice daily (target trough level at POD 0–90 = 6–12 ng/ml, POD 91–365 = 5–8 ng/ml, and POD >366 = 3–7 ng/ml) and MPA 720 mg orally twice daily starting on the day of transplantation.

Table S3). Those patients who developed DSA within 6 weeks post-KTx are considered newly detected memory DSA over true *de novo* DSA.[25,26]

Detection of DSA

Nonheparinized blood was collected to isolate serum for the measurement of anti-HLA-A, -B, -C, -DRB1, DR51/52/53, and -DQB antibodies at all blood sampling time points using the Luminex single-Ag bead assay (One Lambda, Inc., Canoga Park, CA) as previously described.[27] Results were considered to be positive if DSA MFI ≥ 1000; pattern at MFI 400–999; and negative if MFI < 399. All positive DSA samples were subsequently tested for C1q to exclude any prozone effect.

Phenotypic Analyses of T-Cell Subsets by Flow Cytometry

Whole-blood aliquots were incubated with a mixture of monclonal Abs: anti-CD3, -CXCR5, -CD4, -CXCR3, -CD25 (BD, San Jose, CA) and -CD45RO, -PD1, -CD62L, CD127 (eBioscience, San Diego, CA), in the dark for 30 minutes at room temperature. Samples were then incubated with red blood cells lysis buffer (BD) for 10 minutes at room temperature, washed twice, and fixed with fixation/permeabilization buffer (eBioscience) for 40 minutes at 4 °C. For T regulatory cells (T_{REG}) and Ki67 detection, cells were further permeabilized with permeabilization buffer (eBioscience) and incubated in the dark for 30 minutes at 4 °C with anti-FOXP3 and

Table 1. Cohort demographics and clinical events

	Healthy control (n = 13)	Thymoglobulin (n = 31)	Basiliximab[a] (n = 20)	P
Age at Tx, yr (mean ± SD)	51.2 ± 12.4	53.3 ± 12.7	53.8 ± 15.6	0.847
Female, n (%)	6 (46)	16 (52)	4 (20)	0.074
Caucasian, n (%)	13 (100)	26 (84)	17 (85)	0.392
HLA mismatches[b] (mean ± SD)	NA	6.7 ± 2.1	6.6 ± 2.8	0.874
T-FCXM positive, n (%)	NA	0 (0)	0 (0)	–
B-FCXM positive, n (%)	NA	0 (0)	0 (0)	–
PRA I and/or II >20%, n (%)	NA	3 (10)	0 (0)	0.270
History of pregnancies pre-KTx,[c] n (%)	4 (67)	15 (94)	2 (50)	0.062
History of transfusion pre-KTx, n (%)	NA	11 (35)	3 (15)	0.198
DSA post-Tx, n (%)	NA	9 (29)	3 (15)	0.323
TCMR, n (%)	NA	5 (16)	6 (30)	0.304
TAC trough level (μg/l)[d] (mean ± SD)	NA	10.6 ± 2.6	10.0 ± 4.1	0.660
Corticosteroid use,[d] n (%)	NA	7 (22)	6 (30)	0.743

B-FCXM, B-cell flow cytometry cross-match; DSA, donor-specific antibody; KTx, kidney transplant; NA, nonapplicable; PRA I, percent reactive antigen class I; PRA II, percent reactive antigen class II; TAC, tacrolimus; TCMR, T-cell–mediated rejection grade Banff ≥1A; T-FCXM, T-cell flow cytometry cross-match; Tx, transplant.
[a]In the basiliximab group, samples from (i) 3 patients were used only for the pre-Tx analysis as they received thymoglobulin <30 days post-Tx due to rejection; (ii) 6 patients were used only for post-Tx analysis as their pre-Tx samples were collected after mycophenolic acid preload.
[b]HLA mismatches: A, B, C, DRB1, DR51/52/53, DQB alleles.
[c]Within female population.
[d]Measurements at the time of immunological cross-sectional analysis.

anti-Ki67 (eBioscience), washed twice, and immediately acquired. All events were acquired using a Fortessa (BD) cytometer and analyzed with FlowJo software (Tree Star, Ashland, OR). In addition, we applied t-distributed Stochastic Neighbor Embedding algorithm (FlowJo) and integrated the fluorescence intensity of phenotypic markers into a consensus map to visualize the overall differences of cT_{FH} cell subset composition measured by cell cluster density.

Cytokine Determination in Plasma

Cytokine measurements were performed using Luminex bead-based assays at the University of Pittsburgh Luminex Core Laboratory (P30CA047904). Kits including interleukin (IL)-12p70, IL-27, IL-10, IFN-γ, IL-6, IL-17a, IL-21, and IL-23 were purchased from Millipore (EMD Millipore, Billerica, MA).

Cytokine Determination by Intracellular Staining and Flow Cytometry

Banked frozen responder PBMCs were thawed and rested overnight. Responder PBMCs were stimulated with donor cell lysate at 1:5 ratio for 6 hours in the presence of Golgi-plug (BD) and Monensin (eBioscience) at 37 °C, 5% CO_2. Cells were then washed, and surface stained with anti-CD3 (Biolegend, San Diego, CA), -CD8, -CXCR5, (BD) for 20 minutes at 4 °C, washed, and fixed with 1% paraformaldehyde (Sigma, St. Louis,

Table 2. Pre- and post-Tx characteristics of DSA

Patient ID	Induction	Gender	Pre-Tx[a]	Pre-Tx (allele/MFI)[b]	First occurrence post-Tx days[c]	DSA Post-Tx (allele/MFI)	Course of DSA[d]	Clinical manifestation[e]
REC-032	Thymo	M	Negative	–	270	B8/2200; DR4/2285; DR53/3430; DQ8/3713	Persistent	ABMR+TCMR
REC-048	Thymo	M	Negative	–	30	A24/5075	Transient	Asymptomatic
REC-061	Thymo	F	Negative	–	30	DQ7/1100	Transient	ABMR
REC-077	Thymo	M	Negative	–	270	DRB3/1115	Transient	Asymptomatic
REC-081	Thymo	F	Positive	A3/1893	30	A3/7985	Persistent	Asymptomatic
REC-082	Thymo	F	Negative	–	30[f]/180	B45/1071	Persistent	ABMR+TCMR
REC-087	Thymo	M	Pattern	A2/490	30	A2/1262	Transient	Asymptomatic
REC-091	Thymo	F	Negative	–	180	DQ2/2093	Persistent	Asymptomatic
REC-093	Thymo	F	Pattern	B7/653	30	B7/4963	Transient	Asymptomatic
REC-037	Basi	M	Negative	–	360	DQ6/2536	Transient	Asymptomatic
REC-038	Basi	M	Pattern	DRB3/414	90	DRB3/1262	Persistent	ABMR+TCMR
REC-044	Basi	M	Negative	–	270	DQ2/3330	Persistent	ABMR+TCMR

ABMR, antibody-mediated rejection; Basi, basiliximab; DSA, donor-specific antibody; F, female; M, male; MFI, mean fluorescence intensity; TCMR, T-cell–mediated rejection; Thymo, thymoglobulin; Tx, transplant
[a]Negative 0–399 MFI; Pattern 400–999 MFI; Positive ≥ 1000 MFI.
[b]Dash indicates no detectable pre-Tx DSA (none).
[c]DSA first occurrence in the serum at time of research sampling.
[d]Course of DSA within the first year follow-up. Transient = only 1 time positive.
[e]Asymptomatic DSA: patients with DSA-positive in peripheral blood without change in creatinine, glomerular filtration rate, or biopsy-proven ABMR. ABMR ± TCMR: patients with biopsy-proven diagnosis of antibody or T-cell–mediated rejection.
[f]Patient presented with ABMR, however, DSA-negative in peripheral blood.

MO) for 40 minutes. Subsequently, the cells were permeabilized and incubated with mouse serum (Invitrogen, Frederick, MD) for 5 minutes at room temperature, followed by anti-CD40L (eBioscience) and IL-21 monclonal Abs (BD) for 30 minutes at room temperature. Cell were washed and immediately acquired as described previously.

Statistical Analysis

Differences across demographic variables were tested with Fisher exact (for categorical variables), whereas for continuous variables, Student *t* test and 1-way analysis of variance were used. To evaluate differences for cross-sectional data, mean ± SEM were calculated and compared across groups (HC vs. thymoglobulin; HC vs. basiliximab; thymoglobulin vs. basiliximab) using the 2-tailed Student *t* test or Mann-Whitney test according to data distribution. To evaluate group differences between thymoglobulin and basiliximab over time (longitudinal data), and the effect of time within each group, we used a linear mixed model with a random intercept to account for within-subject correlation over time and indicator variables for the treatment at each time point. Mean ± SEM was calculated at each time point and differences from baseline (for each time point within each treatment group) were assessed using linear regression. All results were considered statistically significant if the *P* value was ≤ 0.05.

RESULTS

cT_{FH} Cells With Resting Memory Phenotype Can Be Detected in Peripheral Blood of Patients With ESRD

Pre-Tx patients with ESRD were phenotypically analyzed to detect cT_{FH} cells. The gating strategy to detect cT_{FH} cells ($CD45RO^+CXCR5^+CD4^+CD3^+$), their memory subset distribution (i.e., effector memory (EM): $CD45RO^+CD62L^-$ vs. central memory (CM): $CD45RO^+CD62L^+$), activation status (PD-1), proportion of $CXCR3^+$ (Th1) versus $CXCR3^-$ (Th2+Th17) cT_{FH} cells, and of overall data are shown in Figure 2a–d. Results demonstrate that patients with ESRD display similar levels of $CD45RO^+CD4^+CD3^+$ T cells and of cT_{FH} cells as HC (Figure 2b), dominated by CM (Figure 2b), $CXCR5^+PD\text{-}1^{lo}$ quiescent phenotype (Figure 2c) and with comparable levels of circulating Th1- and Th2+Th17-cT_{FH} cells (Figure 2d). Taken together, these data demonstrate that patients with ESRD and HC have comparable levels of resting memory cT_{FH} with similar polarization.

Interestingly, when patients with ESRD were divided into those who developed DSA post-KTx and those who maintained stable post-KTx, independent of induction therapy, patients who developed DSA post-KTx presented significantly lower % of cT_{FH} compared with stable patients with an elevated EM phenotype compared with HC (Supplementary Figure S1).

Thymoglobulin Induction Triggers Protracted cT_{FH} Cell Depletion, Activation, and Skewed Polarization Toward Th1 Phenotype

The effect of induction therapies on cT_{FH} cell phenotype is not known. Our prospective longitudinal monitoring demonstrates that the absolute numbers of cT_{FH} cells are significantly decreased at all time points post-KTx in the thymoglobulin group as compared with their own pre-KTx values, with those of basiliximab-induced patients, and with HC (Figure 3a). These trends were similar to those of the overall $CD4^+$ T cells (not shown). In contrast, the proportion (%) of cT_{FH} remained unchanged throughout follow-up (Figure 3a).

To determine the levels and kinetics of LIP post-depletion in the thymoglobulin arm, we monitored the proliferation of nondepleted cT_{FH} cells, using Ki-67 staining. Results in Figure 3b show that at 30 days post-KTx, thymoglobulin-induced patients display greater percentage of Ki-67^+ cT_{FH} cells as compared with their own pre-KTx values ($P < 0.001$), and with those of HC or basiliximab-induced patients ($P < 0.0001$), but those values declined to pre-KTx values by 90 days. Interestingly, this was similar to the LIP kinetics observed in total $CD4^+$ T-cell population (Figure 3b). As expected, cT_{FH} and total $CD4^+$ T cells from basiliximab-induced patients did not undergo LIP (Figure 3b).[19]

The cT_{FH} cell memory phenotype was significantly skewed from CM toward EM in the thymoglobulin group compared with basiliximab-induced patients who maintained their memory profiles similar to those of HC (Figure 3c). In addition, cT_{FH} cells from thymoglobulin-induced patients displayed significant upregulation of PD-1 expression from low to intermediate at all time points or high at 90 and 180 days post-depletion compared with their own pre-KTx levels, with those of the basiliximab group and HC (Figure 3d). This elevation in PD-1 expression, accompanied by the decrease in CM suggests that due to LIP, cT_{FH} cells become activated after thymoglobulin induction.

Moreover, while the absolute counts of Th1-cT_{FH} and Th2+Th17-cT_{FH} cells were significantly depleted by thymoglobulin induction, the proportion (%) of these subsets was altered in the circulation of these patients with significant elevation of Th1-cT_{FH} cells (Figure 3e) and a complementary decrease of Th2+Th17-cT_{FH} cells (not shown) throughout follow-up.

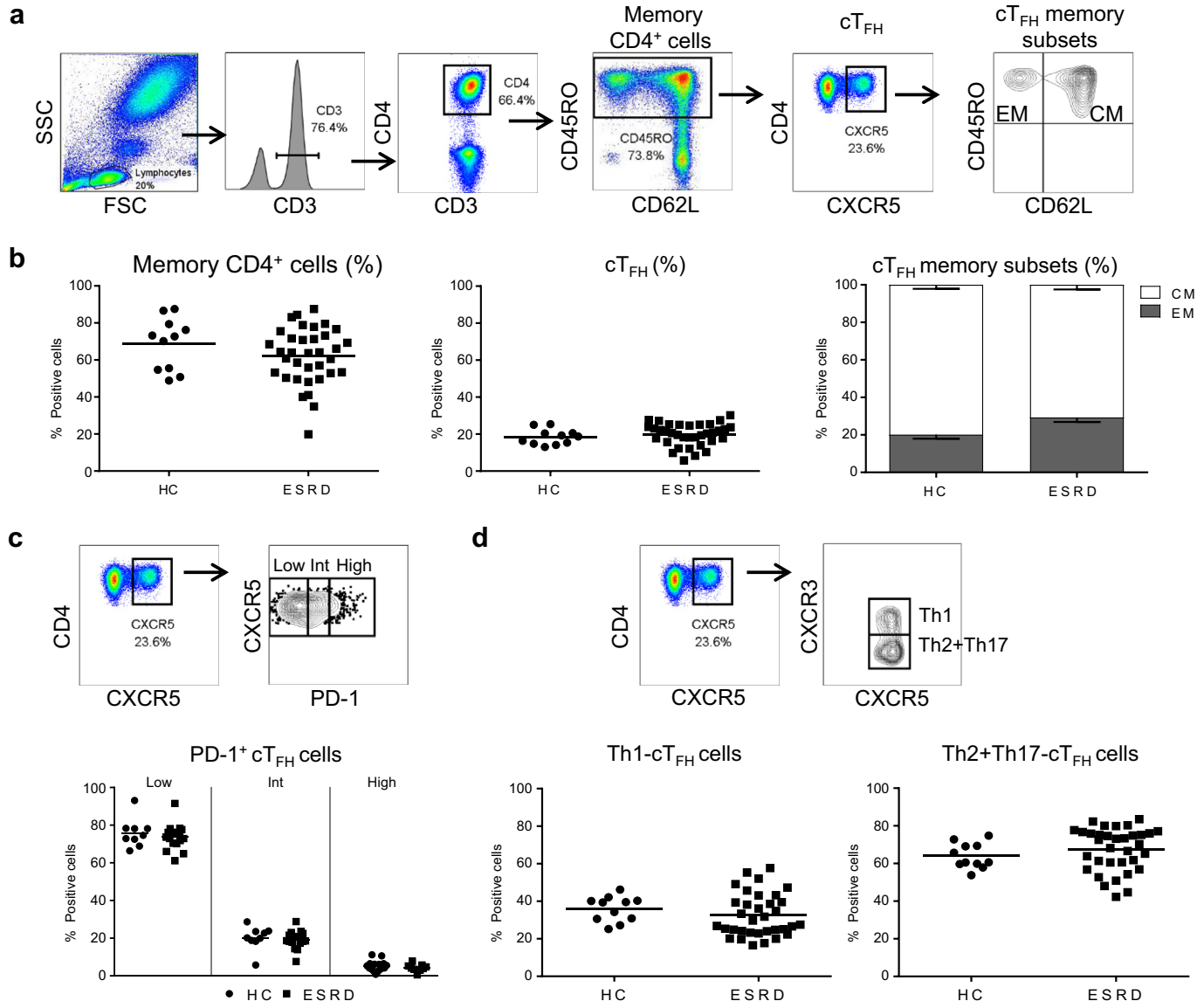

Figure 2. Circulating T follicular helper (cT_{FH}) cells from patients with end-stage renal disease (ESRD) display phenotypic features similar to those of healthy controls (HC). (a) Gating strategy to identify cT_{FH} ($CD45RO^+CXCR5^+CD4^+CD3^+$) and memory phenotype (effector memory [EM]: $CD45RO^+CD62L^-$ and central memory [CM]: $CD45RO^+CD62L^+$). (b) Percentage of overall $CD45RO^+CD4^+$ and cT_{FH} cells, and the mean proportion of EM and CM ± SEM of HC ($n = 13$) and ESRD ($n = 35$). (c) Gating strategy and overall expression of percentage of programmed cell death protein 1 divided into low, intermediate, and high expression on cT_{FH} of HC ($n = 9$) and ESRD ($n = 18$). (d) Identification and the overall percentage of Th1 ($CXCR3^+$) and Th2+Th17 ($CXCR3^-$) within cT_{FH} of HC ($n = 11$) and ESRD ($n = 34$). Each dot represents 1 subject, and the horizontal lines are of the mean values. HC are shown as filled circles, and patients with ESRD are represented by filled squares.

Interestingly, when we performed the longitudinal analyses by type of induction and clinical status post-KTx (DSA^+ vs. stable), we found that in the thymoglobulin-induced group, cT_{FH} cells from DSA^+ KTx recipients had a higher $Ki67^+$ staining (i.e., proliferation) at 30 days as compared with those of stable patients (Supplementary Figure S2A). Conversely, LIP of overall $CD4^+$ T-cell pool did not differ between DSA^+ and stable patients (Supplementary Figure S2A). No elevated $Ki67^+$ was detected in basiliximab-induced patients (Supplementary Figure S2A). In addition, the % EM cT_{FH} cells from DSA^+ patients was significantly higher than those of stable patients (180 and 270 days) in the thymoglobulin group (Supplementary Figure S2B).

Together, these data demonstrate that depleting versus nondepleting induction therapies have different impacts on cT_{FH} cell phenotype post-KTx.

Cross-Sectional Unsupervised t-Distributed Stochastic Neighbor Embedding–Clustering Highlights the Distinct Effect of Induction Therapy on cT_{FH} Cell Phenotype

We next analyzed cross-sectionally the levels and the phenotype of cT_{FH} cell subsets in the first blood sample obtained after DSA occurrence post-KTx (ranging

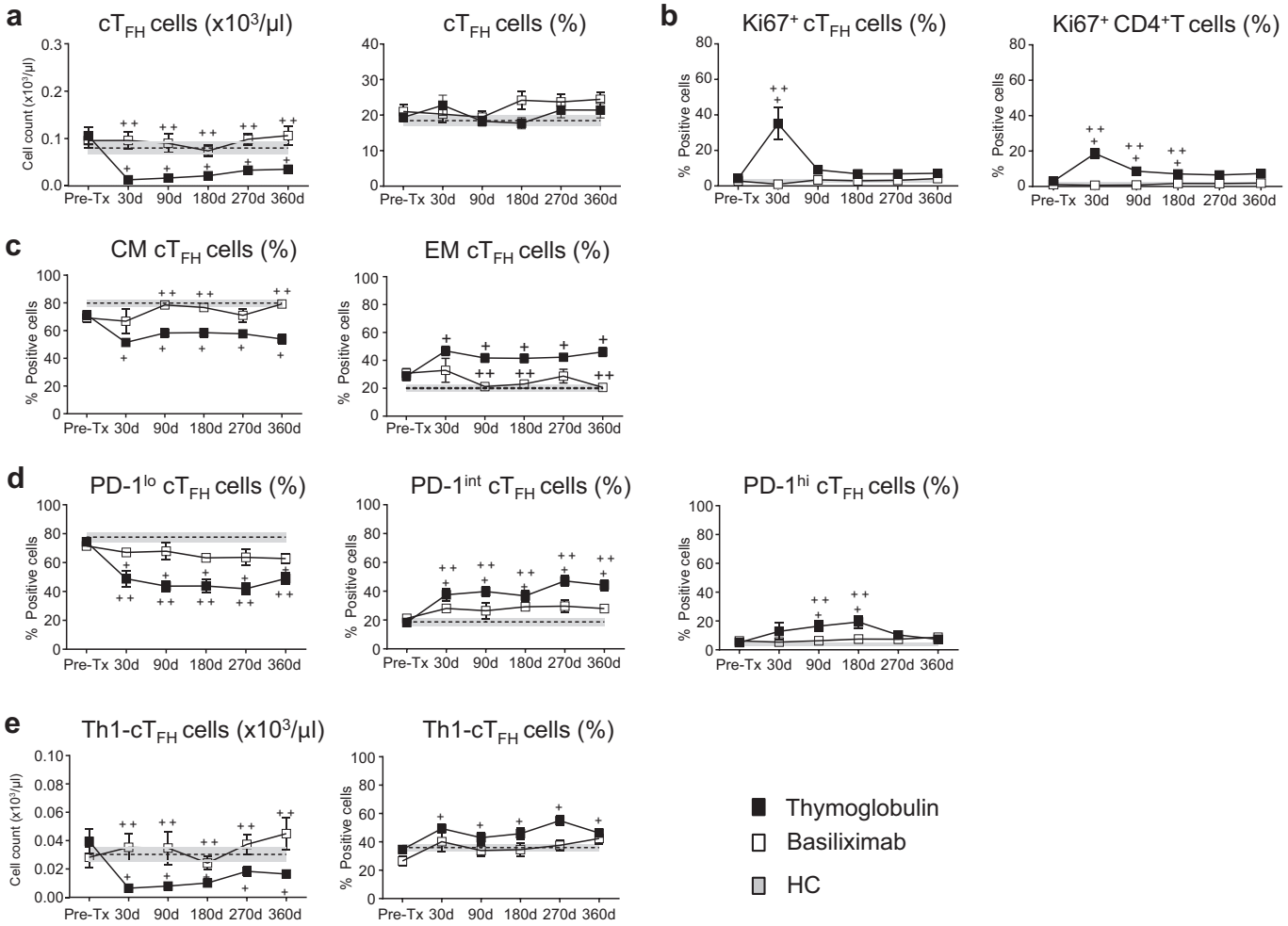

Figure 3. Role of thymoglobulin and of basiliximab induction on circulating T follicular helper (cT$_{FH}$) cells. Kidney transplant (KTx) patients were followed over 1 year with samples collected pre-Tx, 30, 90, 180, 270, and 360 days post-Tx. The longitudinal data for each time point for patients are shown as mean ± SEM. Results from the thymoglobulin group are showed as black filled squares, whereas from the basiliximab cohort as open squares. The values from healthy control (HC) are displayed as dotted lines and gray area displaying mean ± SEM from 1 representative time point. (a) Absolute counts (left) and the percentage (right) of cT$_{FH}$ (CD45RO$^+$CXCR5$^+$CD4$^+$) cells from the thymoglobulin group ($n = 28$), basiliximab group ($n = 17$), and HC ($n = 11$). (b) Percentage of Ki67 expression on cT$_{FH}$ (left) and on total CD4$^+$ T cells (right). Thymoglobulin-induced KTx ($n = 11$), basiliximab-induced KTx ($n = 12$), and HC ($n = 6$). (c) cT$_{FH}$ cell memory distribution as a percentage of central memory (CM) (CD45RO$^+$CD62L$^+$, left) and effector memory (EM) (CD45RO$^+$CD62L$^-$, right) from the thymoglobulin group ($n = 28$), basiliximab group ($n = 17$), and HC ($n = 11$). (d) Programmed cell death 1 (PD-1) expression on cT$_{FH}$ divided into low, intermediate, and high expression from thymoglobulin group ($n = 22$), basiliximab group ($n = 12$), and HC ($n = 11$). (e) Th1-cT$_{FH}$ cells as absolute counts (left) and the percentage (right) from the thymoglobulin group ($n = 38$), basiliximab group ($n = 17$), and HC ($n = 11$). For some of the patients in (a, c–e), some data points are missing. A linear mixed model with a random intercept to account for within-subject correlation over time and indicator variables for the treatment at each time point. Mean ± SEM were further used to calculate differences at each time point across groups using linear regression. $^+$Significant differences ($P = 0.05$–0.0001) within the thymoglobulin group between post-KTx timepoints as compared with their pre-KTx values or to HC values. $^{++}$Significant differences ($P = 0.05$–0.0001) of post-KTx timepoints of thymoglobulin- and basiliximab-induced groups. No difference was found between the basiliximab cohort and HC at any time point.

between 30 and 90 days) (Figures 4 and 5). Peripheral blood of stable patients in both cohorts and HC was used as controls.

The consensus t-distributed Stochastic Neighbor Embedding (tSNE) map generated by concatenating 14 individual maps was overlaid with CXCR3, PD-1, and CD62L markers to further allow, in an unsupervised phenotypic analysis of cT$_{FH}$ cell compartments, the identification of cell clusters with unique phenotypic patterns (Figure 4a).

Subsequently, we de-concatenated the consensus map into 5 group component maps that showed landscapes with unique cell cluster intensities and patterns depending on the group, and with some missing cell clusters in HC and variable cell cluster densities and localization among KTx groups (Figure 4b). Moreover, gating on the highest cell density cluster in each group map, we further compared the CXCR3, PD-1, and CD62L expression from the consensus map (Figure 4a). This concomitant analysis allowed us to conclude that

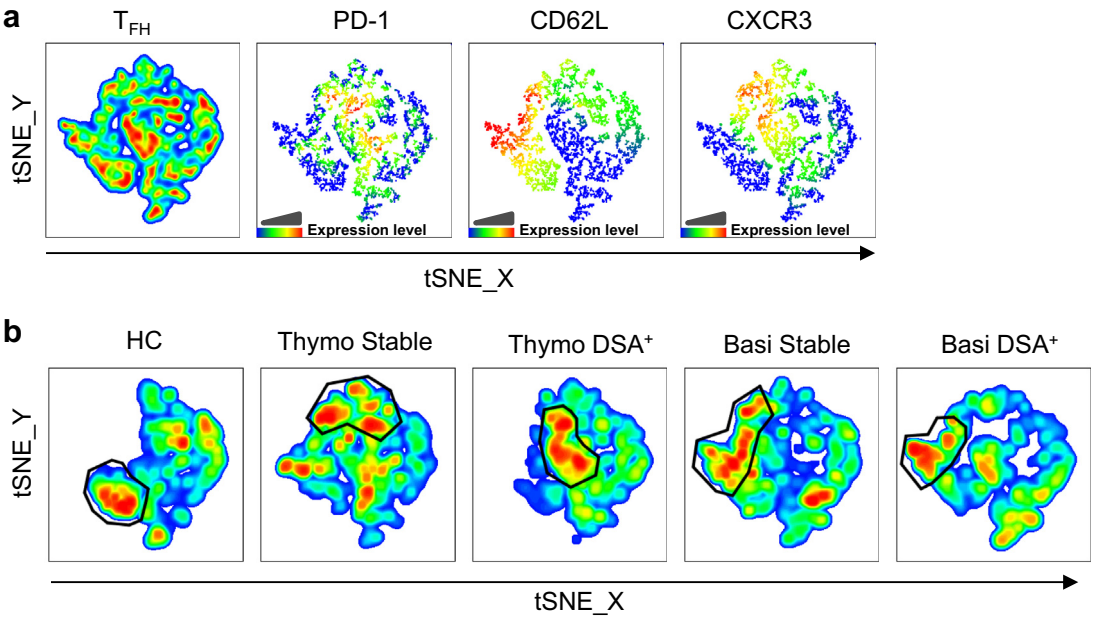

Figure 4. Identification of circulating T follicular helper (cT_{FH}) cell cluster distribution by t-distributed Stochastic Neighbor Embedding (tSNE) reveal that thymoglobulin-induced kidney transplant (KTx) patients who developed donor-specific anti-HLA antibodies (DSA) display elevated effector memory (EM) programmed cell death 1 (PD-1)$^{int/hi}$ Th1-T_{FH} phenotypes. We applied the tSNE algorithm to allow for an unsupervised analysis of cT_{FH} cell compartment. (a) Three representative subjects from each group (exception, basiliximab DSA$^+$ [$n = 2$]), for a total of 14 samples, were normalized to 500 cT_{FH} cells by down sampling (FlowJo) and concatenated into 1 file to create a consensus tSNE map. Different marker (PD-1, CD62L, and CXCR3) fluorescence intensity was identified by color gradient. (b) Clusters with a high concentration of cells with similar phenotypes are highlighted by gating on deconcatenated tSNE for all groups. Basi, basiliximab; HC, healthy control; thymo, thymoglobulin.

in DSA$^+$ thymoglobulin-induced patients, the highest cell density cluster consists of CXCR3$^+$ (Th1), PD1^{hi} (activated) and CD62L$^-$ (EM), whereas in the stable group this consists of CXCR3$^+$ (Th1), PD-1$^{int/hi}$ (semi-activated), CD62L$^{+/-}$ (EM/CM). In contrast, these high-density clusters had different localization on the cT_{FH} cell maps from basiliximab-induced patients or HC and showed instead CXCR3$^{-/+}$ (mixed Th1, Th2, or Th17), PD1$^{low/int}$ (resting) and CD62L$^+$ (CM) (Figure 4).

These data further depict that different induction therapies and clinical status post-KTx can affect cT_{FH} cell phenotype post-KTx.

Two-Dimensional Phenotypic Analyses Confirm That Unlike Basiliximab-Induced KTx Patients, Thymoglobulin-Induced KTx Patients Display Elevated Activated Th1-cT_{FH}

Next, we used the classic 2-dimensional analysis, and confirmed that the % cT_{FH} cells with EM or partially/activated (PD-1$^{int/hi}$) phenotypes was elevated in both stable and DSA$^+$ thymoglobulin-induced patients compared with basiliximab and HC groups, with DSA$^+$ patients displaying the highest significant values (Figures 5a and b). Moreover, the percentage of EM Th1-cT_{FH} cells as well as PD1^{hi}Th1-cT_{FH} was highest in the thymoglobulin-induced DSA$^+$ patients as compared with all other groups (Figure 5c and Supplementary Figure S3). Similar to HC, basiliximab-induced KTx patients presented significantly higher percentage of CM Th2+Th17-cT_{FH} compared with thymoglobulin-induced KTx patients (Figure 5d). Interestingly, the EM component of cT_{FH} and Th1-cT_{FH} were significantly higher in DSA$^+$ patients compared with stable patients in the sample preceding DSA occurrence (data not shown).

To validate our findings, an independent cross-sectional cohort of thymoglobulin-induced patients ($n = 23$) was recruited from UPMC (Supplementary Tables S2 and S3). Results confirmed our previous findings by identifying significantly higher percentage of cT_{FH} cells with EM and PD-1^{hi} phenotypes as well as highest PD1^{hi}Th1-cT_{FH} in DSA$^+$ patients as compared with stable and HC (Supplementary Figure S4).

DSA$^+$ KTx Patients, Regardless of Induction Therapies, Show Increased cT_{FH}/T_{REG} Ratios

It is recognized that effector T-cell responses are tightly modulated by T_{REG}, and that any disturbances of this cell subset may lead to rejection.[28] We therefore assessed the levels of circulating T_{REG} (CD3$^+$CD4$^+$CD25^{hi}CD127$^-$FOXP3$^+$) at the same time points used to monitor cT_{FH} cells. We found that the % T_{REG} was overall decreased in the thymoglobulin group compared with patients in the basiliximab group or to HC (Figure 6a). In addition, DSA$^+$ patients in both cohorts, displayed lower % T_{REG} and higher

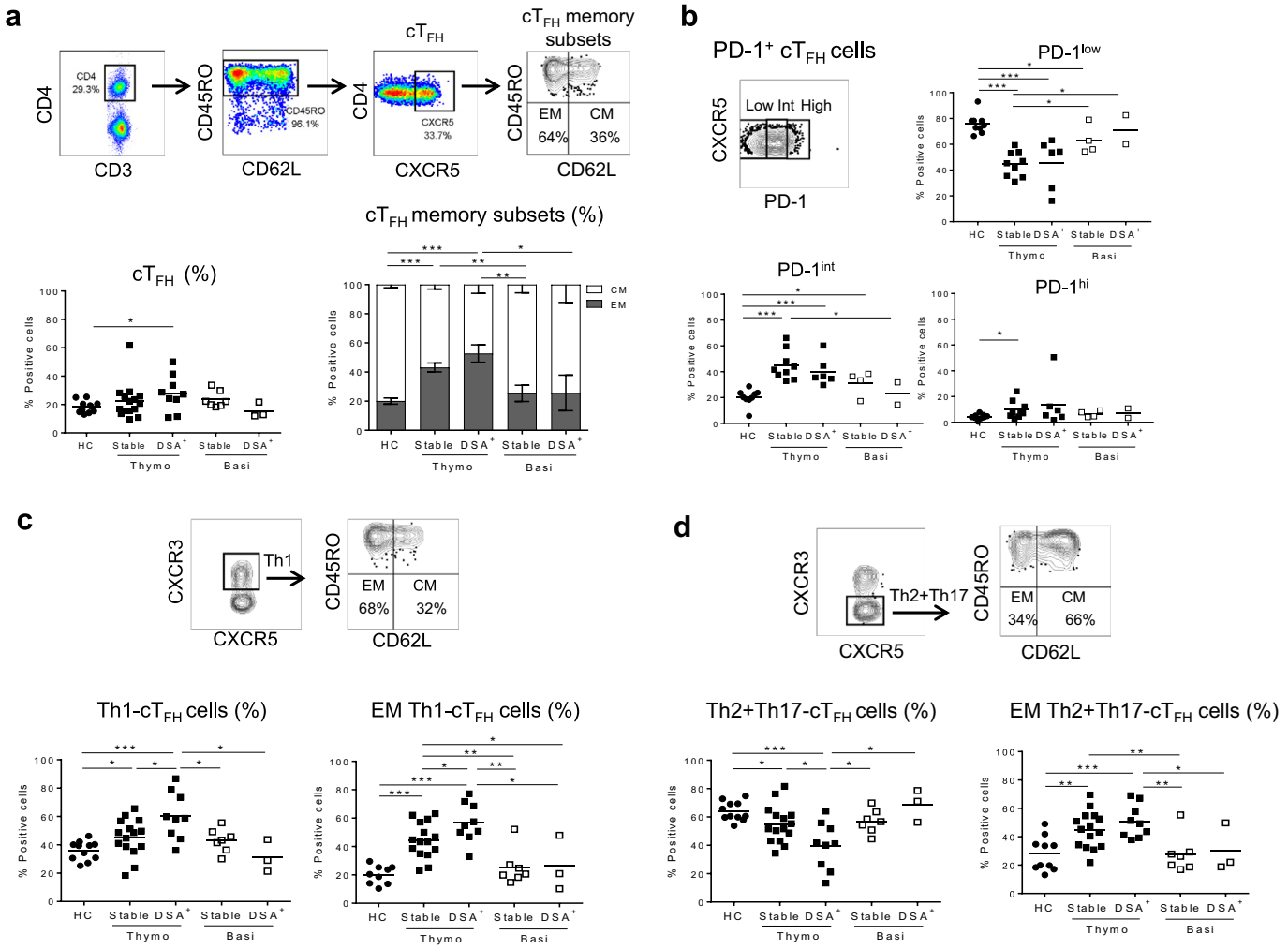

Figure 5. Kidney transplant (KTx) recipients that developed donor-specific anti-HLA antibodies (DSA) display elevated Th1–circulating T follicular helper (cT_{FH}) cells with semi-activated phenotypes. Cross-sectional phenotypic analyses were performed on the first blood sample obtained after DSA detection in the serum. Similar time points were selected for stable patients for comparison. (a) Gating strategy to identify cT_{FH} cells, their overall frequency (left), and their memory distribution of central memory (CM) and effector memory (EM) (right). Healthy controls (HC), $n = 11$; thymoglobulin, stable $n = 15$ and DSA^+ $n = 9$; basiliximab, stable $n = 7$ and DSA^+ $n = 3$. (b) Gating strategy to identify the percentage of programmed cell death 1 (PD-1) expression (low, intermediate, high) on cT_{FH} and overall data (HC, $n = 9$; thymoglobulin, stable $n = 9$ and DSA^+ $n = 6$; basiliximab, stable $n = 4$ and DSA^+ $n = 2$). (c) Gating strategy to identify the frequency of Th1-cT_{FH} cells (left) and of EM distribution (right) and the overall data (HC, $n = 11$; thymoglobulin, stable $n = 15$ and DSA^+ $n = 9$; basiliximab, stable $n = 7$ and DSA^+ $n = 3$). (d) Gating strategy to identify the frequency of Th2+Th17-cT_{FH} cells (left) and of EM distribution (right) and the overall data (HC, $n = 11$; thymoglobulin, stable $n = 15$ and DSA^+ $n = 9$; basiliximab, stable $n = 7$ and DSA^+ $n = 3$). Each dot represents 1 subject, and the horizontal lines are of the mean values. HCs are represented by filled circles, thymoglobulin-induced patients by filled squares, and basiliximab-induced patients by open squares. Two-tailed Student *t* test or Mann-Whitney test was used according to data distribution. $^*P < 0.05$; $^{**}P < 0.01$; $^{***}P < 0.001$.

% Th1-cT_{FH} (thymoglobulin-induced) or Th2+Th17-cT_{FH} (basiliximab-induced) cells. These changes resulted in a significantly higher Th1-cT_{FH}:T_{REG} ratio in DSA^+ thymoglobulin patients and Th2+Th17-cT_{FH}:T_{REG} ratio in basiliximab-induced patients compared with those ratios from stable KTx patient counterparts and HC (Figure 6b).

These results illustrate that the 2 types of induction have different effects on cT_{FH} and T_{REG} phenotypes, but regardless of induction, DSA^+ patients display higher cT_{FH}:T_{REG} ratio.

Patients With ESRD Who Develop DSA Post-KTx Exhibit Pre-KTx Circulating Donor-Specific IL-21^+ cT_{FH} Cells and Increased Plasma Levels of T_{FH} Cell-Promoting Inflammatory Cytokines

We next assessed the proinflammatory cytokine levels in the pre-KTx plasma, and whether cT_{FH} cells reactive to donor HLA-Ag can be detected in the circulation of patients with ESRD, who developed DSA or not post-KTx, independently of the induction therapy. Our results show that patients who developed DSA post-KTx displayed significantly higher levels of IL-12p70,

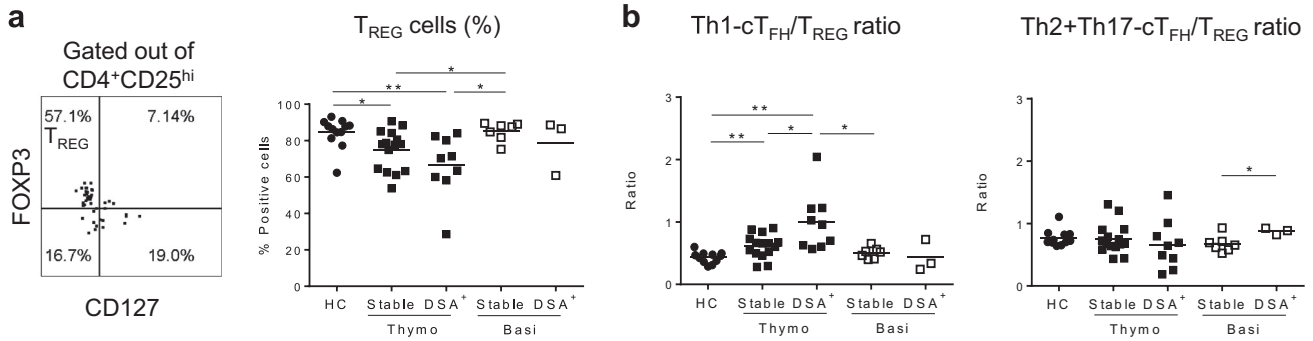

Figure 6. Kidney transplant (KTx) recipients who developed donor-specific anti-HLA antibodies (DSA) display decreased T regulatory (T_{REG}) cells, resulting in an elevated Th1–circulating T follicular helper (cT_{FH})/T_{REG} ratio. Cross-sectional phenotypic analyses were performed on the first blood sample obtained after DSA detection in the serum. Similar time points were selected for stable patients for comparison. (a) Gating strategy and the overall results of the frequency of T_{REG} (healthy controls [HC], $n = 12$; thymoglobulin, stable $n = 15$ and DSA^+ $n = 9$; basiliximab, stable $n = 7$ and DSA^+ $n = 3$). (b) Ratio between the frequency (%) of Th1-cT_{FH} and of T_{REG} (left) and of Th2+Th17-cT_{FH} and of T_{REG} (right) from HC and post-Tx patients (HC $n = 11$; thymoglobulin, stable $n = 15$ and DSA^+ $n = 9$; basiliximab, stable $n = 7$ and DSA^+ $n = 3$). Each dot represents 1 subject, and the horizontal lines are the mean values. HCs are represented by filled circles, thymoglobulin-induced patients by filled squares, and basiliximab-induced patients by open squares. Two-tailed Student *t* test or Mann-Whitney test was used according to data distribution. $*P < 0.05$; $**P < 0.01$.

IL-17a, IL-21, and IL-23 compared with stable patients (Figure 7a). These proinflammatory cytokines are known to promote human T_{FH} cell generation[29] and to shape their fate, suggesting that these programs may be easily activated post-KTx.

To further test whether memory IL-21^+ cT_{FH} cells reactive to donor allo-Ag are detectable in the circulation of patients with ESRD pre-Tx, we set-up short-term (6-hour) stimulation assays consisting of patients' PBMCs pulsed or not with their donor cell lysate. Our results indicate that patients with ESRD who developed DSA post-KTx carried significantly more circulating memory ($CD40L^+IL\text{-}21^+$) cT_{FH} cells before KTx than patients with ESRD who remained stable post-KTx (Figure 7b).

All these results demonstrate that patterns of proinflammatory cytokine milieu favorable for cT_{FH} cell development, as well as concomitant presence of memory allo-reactive IL-21^+ cT_{FH} cells can be detected in ESRD pre-KTx and may suggest increased risk for DSA generation post-KTx. These results also underscore the importance of pre-KTx screening for cellular donor-reactive memory cT_{FH} cells in patients with ESRD.

DISCUSSION

The goal of the current study was to explore the cT_{FH} cell phenotypic changes triggered by induction therapy at KTx and by DSA occurrence. Our results demonstrate that thymoglobulin induction and subsequent LIP triggers significant cT_{FH} cell depletion and homeostatic proliferation accompanied by preferential expansion of Th1-cT_{FH} with EM and PD-1 upregulation. Furthermore, in thymoglobulin-induced patients, the activated Th1-cT_{FH} repopulation post-KTx and the increased Th1-cT_{FH}:T_{REG} ratio correlate with DSA occurrence. Conversely, in the basiliximab group, the Th2+Th17-cT_{FH}:T_{REG} ratio was changed at DSA occurrence. These underscore different mechanisms of cT_{FH}/T_{REG} homeostasis post-KTx triggered by different induction therapies and the presence or absence of LIP.

Because our analyses revealed that LIP and subsequent repopulation of the thymoglobulin-resistant cT_{FH} cells specifically lowered their threshold for activation and thus may render them susceptible targets to donor-Ag specific trigger, we postulate that long-term post-KTx, if under-immunosuppressed (during weaning) or if noncompliant, thymoglobulin-induced patients may be vulnerable to DSA generation due to the persistence of activated cT_{FH} cell phenotype.

Most randomized clinical studies so far have investigated the role of induction therapies on cellular rejection. These studies concluded that depleting therapy preferentially benefits sensitized KTx candidates by lowering T-cell–mediated rejection occurrence post-Tx compared with nondepleting induction therapies.[18,30–34] However, the role of induction therapy on DSA occurrence is not well understood.[35] The very few published data on this topic resulted from single-center, nonrandomized clinical studies, with poor definition of *de novo* versus memory DSA status, and with variable clinical follow-up. In one study, the authors compared the T-cell depleting induction used in desensitized moderate risk patients with nondepleting induction used in low-risk patients.[36] Another single-center study reported DSA incidence in patients grouped together, regardless of their induction therapy.[37] Therefore, none of these studies are yet

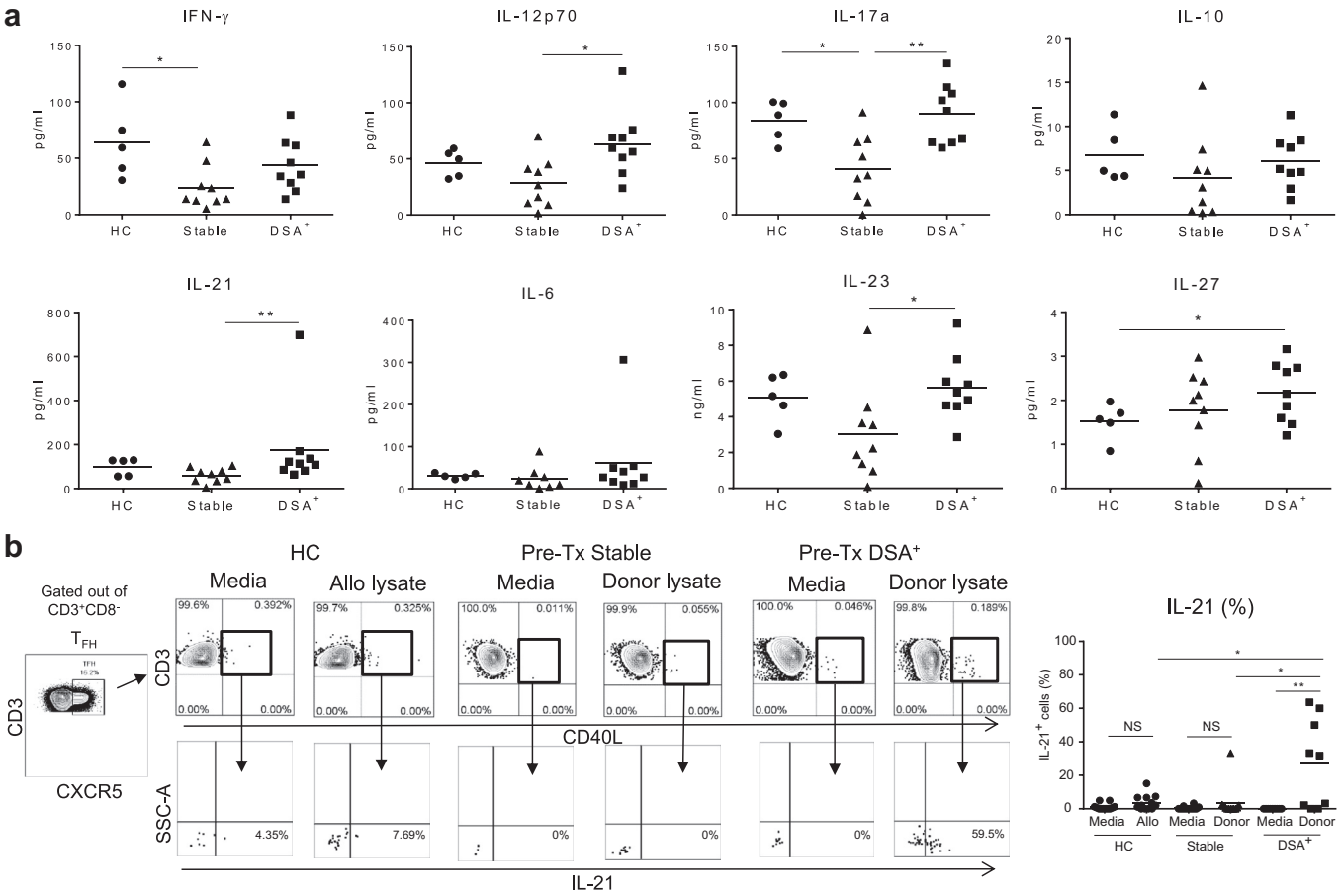

Figure 7. Patients with end-stage renal disease (ESRD) who develop donor-specific anti-HLA antibodies (DSA) after kidney transplant (KTx) carry pre-KTx allo-reactive interleukin (IL)-21$^+$ circulating T follicular helper (cT$_{FH}$) T cells and cT$_{FH}$ cell-promoting inflammatory cytokines in the plasma. (a) Luminex cytokine analyses were performed retrospectively in the plasma of patients with ESRD who either remained stable ($n = 9$) or developed DSA ($n = 9$) post-KTx, and in plasma of healthy controls (HC) ($n = 5$). Each panel displays 1 single cytokine as indicated. (b) Gating strategy cT$_{FH}$CD40L$^+$ to detect IL-21-producing cells is shown. These were quantified by intracellular staining and flow cytometry at the end of a short (6-hour) stimulation with cell lysate–containing allo-antigen (Ag) (HC) or donor-Ag (ESRD). Overall IL-21$^+$ cT$_{FH}$ cell data are displayed for patients with ESRD (Stable $n = 12$, DSA$^+$ $n = 9$) and HC ($n = 12$). Each dot represents 1 subject, and the horizontal lines are the mean values. HCs are represented by filled circles, patients with ESRD who remained stable post-KTx by filled triangles, and those who developed DSA post-Tx by filled squares. Two-tailed Student *t* test or Mann-Whitney test was used according to data distribution. *$P < 0.05$; **$P < 0.01$. NS, nonsignificant; IFN, interferon.

conclusive. Although our current study was not designed or powered to correlate the induction therapy with the incidence of DSA, it showed that thymoglobulin induction, unlike basiliximab, did significantly expand the proportion of activated cT$_{FH}$ cell with Th1 phenotypes. This suggests that LIP and subsequent early repopulation of the thymoglobulin-resistant cT$_{FH}$ cells specifically lowered their threshold for activation and thus rendered them susceptible targets to donor-Ag specific trigger if memory to donor (pre-Tx IL-21$^+$ cT$_{FH}$ testing) is present. We further postulate that long-term post-KTx, if under-immunosuppressed (i.e., during weaning or noncompliant), thymoglobulin-induced patients may be also vulnerable to DSA generation due to the persistence of activated cT$_{FH}$ cell phenotype for at least 1 year post-Tx per our follow-up, and therefore should be closely monitored post-Tx. In a recent study, Hricik *et al.*[38] found that tacrolimus withdrawal in immune quiescent thymoglobulin-induced KTx recipients (with no history of DSA) had to be terminated prematurely because of unacceptable rates of *de novo* DSA occurrence in the tacrolimus withdrawal arm versus nonweaning. Although that was not a randomized prospective study to test DSA incidence after weaning in patients receiving or not induction therapy, our hypothesis is that those patients who developed DSA after weaning might have presented activated donor-specific cT$_{FH}$ precursors that were otherwise well controlled by tacrolimus.[17]

In a recent publication, Chen *et al.*[23] showed that after thymoglobulin induction, maintenance immunosuppression only partially reduced CD40L and ICOS expression on CD3/CD28 activated cT$_{FH}$ *ex vivo* , and with no effect on IL-21 secretion, suggesting an inadequate block on T$_{FH}$ helper function by those drugs. Therefore, monitoring for the presence of activated

donor-specific cT_{FH} cells might be a critical step before weaning, but its importance still remains to be established in future studies.

Interestingly, de Graav *et al.*[39] found in a cohort of basiliximab-induced KTx patients that the absolute numbers of total cT_{FH} (not only $CD45RO^{+}cT_{FH}$) post-KTx were the highest in patients with preformed DSA (>5000 MFI cutoff), and when isolated, cT_{FH} preserved their ability to provide IL-21–mediated B-cell help. Cano-Romero *et al.*[40] showed a role for different induction therapies on cT_{FH} cells after KTx. Although their findings on the role of induction therapies on cT_{FH} cells concur with our results reported here, the further focus of our studies diverged. We assessed the relationship of cT_{FH} cells with DSA (donor-Ag specific responses) post-KTx, whereas they studied the relationship of cT_{FH} cells with anti-HLA sensitization (not donor-Ag specific responses).[40] Therefore, future studies should consider standardization of cT_{FH} cell gating strategy, distinction between HLA-Ab and DSA, and the threshold of DSA positivity.

The skewed representation of cT_{FH} cell subsets that are differently modulated by induction therapy is important given the distinct ability of cT_{FH} cell subsets to help B cells, and subsequently shape Ab responses.[41] The literature provides evidence that Th1-cT_{FH} cells can primarily help memory B-cell differentiation into IgG-secreting plasmablasts, but are poor helpers for naïve B-cell differentiation, and thus are considered suboptimal helpers, unlike Th2- or Th17-cT_{FH} cells who can help both naïve and memory B cells.[42]

The effect of depleting versus nondepleting agents on T_{REG} has been previously studied.[20,43] In addition, published data suggest that T_{FH} cell responses may be tightly modulated by T_{REG}.[44] Our cross-sectional data indicate that differently polarized cT_{FH} cells regardless of the induction therapy used may be regulated by T_{REG}, suggesting that the T_{REG} cells present in the circulation of patients decrease at DSA occurrence.

Our results underscore the potential importance of cellular monitoring for cT_{FH} to enhance the detection of possible donor-Ag specific humoral sensitization pre-KTx. Currently available methods to detect humoral sensitization consist of measurements of circulating anti-HLA Abs in patients' serum. Methods for monitoring recipients' T cellular allo-reactivity using PBMCs with IFN-γ enzyme-linked immunosorbent spot or intracellular staining and flow cytometry against a panel of allo-Ag or against donor-Ag have been previously developed and can identify patients at risk of cellular rejection post-KTx.[45–47] These assays do not address the issue of humoral sensitization and thus are not specific to detect the donor-Ag specific memory cT_{FH} cell (and B-cell) pools. Therefore, "personalized" pre-Tx cellular screening for donor-Ag specific memory B cells[48,49] or as reported here for donor-Ag specific $IL\text{-}21^{+}cT_{FH}$ cellular presensitization, may be of great value for identifying low-risk patients who may develop DSA post-KTx. Such patients with $cT_{FH}IL21^{+}$ pre-Tx should be monitored closely post-KTx to avoid long-term DSA occurrence, or should not be weaned and be considered for Belatacept induction.[50,51]

We selected IL-21 for identifying humoral sensitization because it is the signature cytokine for functional T_{FH} cells, critical for B-cell help and Ab responses, including allo-Ab/DSA responses.[52,53] In addition to cellular screening, our results show that enzyme-linked immunosorbent assay monitoring of pre-KTx plasma may detect elevated T_{FH} cell-friendly inflammatory cytokines in recipients who developed DSA post-KTx, as compared with those who remained stable. Inflammatory cytokines (IL-12p70, IL-21, IL-6, IL-17a) that shape T_{FH} cell induction, polarization, and maintenance have been previously described.[29] These pre-Tx screenings in conjunction with measuring cT_{FH} cell proliferation ($Ki67^{+}$) in thymoglobulin-induced patients in the first 3 months post-Tx may specifically identify patients at risk for DSA occurrence. Interestingly, this distinct kinetics of memory cT_{FH} cell repopulation in DSA^{+} versus DSA^{-} patients suggests a role for cT_{FH} T-cell receptor stimulation by donor-Ag/major histocompatibility complex class II in addition to cytokine stimulation.[54] All these potential clinically relevant tests need further validation on a larger number of patients to confirm their robustness and reliability in identifying correlations among induction therapy, memory cT_{FH}, and DSA occurrence.

In conclusion, (i) thymoglobulin induction triggers protracted cT_{FH} cell depletion, activation, and skewed polarization toward the Th1 phenotype compared with basiliximab induction; (ii) DSA^{+} KTx patients, regardless of induction therapies, show increased cT_{FH}/T_{REG} ratios; (iii) patients with ESRD who develop DSA post-KTx exhibit pre-Tx circulating donor-specific memory $IL\text{-}21^{+}$ cT_{FH} cells and increased plasma levels of T_{FH} cell-promoting inflammatory cytokines. Thus, future randomized controlled clinical trials to validate the present study should implement donor-Ag specific screening for detection of cellular presensitization (memory $cT_{FH}/B/T_{REG}$), measurements of inflammatory cytokines for cT_{FH} cell, and monitoring of Ki67 proliferation (for thymoglobulin induction) in addition to DSA measurements and characterization.

DISCLOSURE

All the authors declared no competing interests.

ACKNOWLEDGMENTS

The authors thank the patients, donors, and nurses from The Christ Hospital and from the University of Cincinnati, for making this study possible. This work was supported by the following grants: R01-AI096553 (FGL); R21-AI116746 (DM), and R01 AI130010 (DM) and by the Human Immunology Program at the Starzl Transplantation Institute.

SUPPLEMENTARY MATERIAL

Figure S1. cT_{FH} memory distribution in patients with ESRD who developed or not DSA post-KTx independently of induction therapy. (**A**) % of overall memory ($CD45RO^+CD4^+$), cT_{FH} cells, and the mean proportion of EM and CM ± SEM of HC (n = 11), ESRD-Stable (n = 26), and ESRD-DSA^+ (n = 9). (**B**) Overall expression of % PD-1 divided into low, intermediate, and high expression on cT_{FH} of HC (n = 9), ESRD-Stable (n = 13), and ESRD-DSA^+ (n = 5). (**C**) Overall % of Th1 ($CXCR3^+$) and Th2+Th17 ($CXCR3^-$) within cT_{FH} of HC (n = 11), ESRD-Stable (n = 26), and ESRD-DSA^+ (n = 8). Each dot represents 1 subject, and the horizontal lines are of the mean values. HC are shown as filled circles, whereas ESRD-Stable patients are represented by filled triangles and ESRD-DSA^+ by filled squares. Two-tail Student *t* test or Mann-Whitney test were used according to data distribution. $*P < 0.05$.

Figure S2. Longitudinal data from DSA^+ versus stable Tx recipients from thymoglobulin- and basiliximab-induced patients. The longitudinal data for each time point from patients are shown as mean ± SEM. Results from DSA^+ patients are shown as black filled squares, whereas from stable patients as black filled triangles. (**A**) Percentage of Ki67 expression on cT_{FH} (left panel) and on total $CD4^+$ T cells (right panel). Thymoglobulin-induced KTx patients (Stable n = 7, DSA^+ n = 9) and Basiliximab-induced KTx patients (Stable n = 11, DSA^+ n = 3). (**B**) cT_{FH} cell memory distribution is represented as the percentage of CM ($CD45RO^+CD62L^+$, left panel) and EM ($CD45RO^+CD62L^-$, right panel) from the Thymoglobulin group (DSA^+ n = 8, Stable n = 14). For some of the patients in Panels **A** and **B** some data points are missing. $*P < 0.05$.

Figure S3. KTx recipients that developed DSA post-Tx display elevated PD-$1^{hi}CXCR3^+$-cT_{FH} cells. Cross-sectional phenotypic analyses were performed on the first blood sample obtained after DSA detection in the serum. Similar time points were selected for stable patients for comparison. Gating strategy to identify the percentage of PD-$1^{hi}CXCR3^+$ on cT_{FH} and overall data (HC: n = 7; Thymoglobulin group: Stable n = 8, and DSA^+ n = 6; Basiliximab group: Stable n = 5, and DSA^+ n = 2). Each dot represents 1 subject, and the horizontal lines are of the mean values. HC are represented by filled circles, Thymoglobulin-induced patients by filled squares, and Basiliximab-induced patients by open squares. Two-tail Student *t* test or Mann-Whitney test were used according to data distribution. $*P < 0.05$.

Figure S4. Elevated PD1^{hi}Th1-cT_{FH} with EM phenotype results were confirmed in an independent cohort of thymoglobulin-induced KTx patients from UPMC. Cross-sectional phenotypic analyses were performed on the first blood sample obtained after DSA detection in the serum. Similar time points were selected for stable patients for comparison. (**A**) Mean ± SEM of cT_{FH} cells memory distribution CM and EM (HC, n = 9; Stable, n = 10; DSA^+, n = 7). (**B**) Overall percentage of PD-1 expression (low, intermediate, and high) on cT_{FH} (HC, n = 9; Stable, n = 9; DSA^+, n = 7). (**C**) Overall percentage of PD-$1^{hi}CXCR3^+$ on cT_{FH} (HC, n = 7; Stable, n = 9; DSA^+, n = 7). Each dot represents 1 subject, and the horizontal lines are of the mean values. HC are represented by filled circles, Thymoglobulin-induced stable patients by filled triangles and DSA^+ patients by filled squares. Two-tail Student *t* test or Mann-Whitney test were used according to data distribution. $*P < 0.05$; $**P < 0.01$; $***P < 0.001$.

Table S1. Etiologies of ESRD.

Table S2. UPMC cohort: demographics and clinical events.

Table S3. UPMC cohort: DSA characteristics.

Supplementary material is linked to the online version of the paper at www.kireports.org/.

REFERENCES

1. Terasaki PI, Ozawa M. Predicting kidney graft failure by HLA antibodies: a prospective trial. *Am J Transplant*. 2004;4:438–443.
2. Gaston RS, Cecka JM, Kasiske BL, et al. Evidence for antibody-mediated injury as a major determinant of late kidney allograft failure. *Transplantation*. 2010;90:68–74.
3. Loupy A, Hill GS, Jordan SC. The impact of donor-specific anti-HLA antibodies on late kidney allograft failure. *Nat Rev Nephrol*. 2012;8:348–357.
4. Reed EF. Mechanisms of action and effects of antibodies on the cells of the allograft. *Hum Immunol*. 2012;73:1211–1212.
5. Wiebe C, Nickerson P. Posttransplant monitoring of de novo human leukocyte antigen donor-specific antibodies in kidney transplantation. *Curr Opin Organ Transplant*. 2013;18:470–477.
6. Lefaucheur C, Viglietti D, Bentlejewski C, et al. IgG donor-specific anti-human HLA antibody subclasses and kidney allograft antibody-mediated injury. *J Am Soc Nephrol*. 2016;27:293–304.
7. Leffell MS, Zachary AA. Anti-allograft antibodies: some are harmful, some can be overcome, and some may be beneficial. *Discov Med*. 2010;9:478–484.
8. McHeyzer-Williams LJ, Pelletier N, Mark L, et al. Follicular helper T cells as cognate regulators of B cell immunity. *Curr Opin Immunol*. 2009;21:266–273.
9. King C, Tangye SG, Mackay CR. T follicular helper (TFH) cells in normal and dysregulated immune responses. *Annu Rev Immunol*. 2008;26:741–766.

10. Chevalier N, Jarrossay D, Ho E, et al. CXCR5 expressing human central memory CD4 T cells and their relevance for humoral immune responses. *J Immunol*. 2011;186:5556–5568.
11. Schmitt N, Ueno H. Blood Tfh cells come with colors. *Immunity*. 2013;39:629–630.
12. Morita R, Schmitt N, Bentebibel SE, et al. Human blood CXCR5(+)CD4(+) T cells are counterparts of T follicular cells and contain specific subsets that differentially support antibody secretion. *Immunity*. 2011;34:108–121.
13. He J, Tsai LM, Leong YA, et al. Circulating precursor CCR7(lo) PD-1(hi) CXCR5(+) CD4(+) T cells indicate Tfh cell activity and promote antibody responses upon antigen reexposure. *Immunity*. 2013;39:770–781.
14. Reinhardt RL, Liang HE, Locksley RM. Cytokine-secreting follicular T cells shape the antibody repertoire. *Nat Immunol*. 2009;10:385–393.
15. Bentebibel SE, Lopez S, Obermoser G, et al. Induction of ICOS+CXCR3+CXCR5+ TH cells correlates with antibody responses to influenza vaccination. *Sci Transl Med*. 2013;5:176ra132.
16. Le Coz C, Joublin A, Pasquali JL, et al. Circulating TFH subset distribution is strongly affected in lupus patients with an active disease. *PloS One*. 2013;8:e75319.
17. Pearl JP, Parris J, Hale DA, et al. Immunocompetent T-cells with a memory-like phenotype are the dominant cell type following antibody-mediated T-cell depletion. *Am J Transplant*. 2005;5:465–474.
18. Toso C, Edgar R, Pawlick R, et al. Effect of different induction strategies on effector, regulatory and memory lymphocyte sub-populations in clinical islet transplantation. *Transpl Int*. 2009;22:182–191.
19. Bouvy AP, Kho MM, Klepper M, et al. Kinetics of homeostatic proliferation and thymopoiesis after rATG induction therapy in kidney transplant patients. *Transplantation*. 2013;96:904–913.
20. Gurkan S, Luan Y, Dhillon N, et al. Immune reconstitution following rabbit antithymocyte globulin. *Am J Transplant*. 2010;10:2132–2141.
21. Metes DM. T follicular helper cells in transplantation: specialized helpers turned rogue. *Transplantation*. 2016;100:1603–1604.
22. Walters GD, Vinuesa CG. T follicular helper cells in transplantation. *Transplantation*. 2016;100:1650–1655.
23. Chen CC, Koenig A, Saison C, et al. CD4+ T cell help is mandatory for naive and memory donor-specific antibody responses: impact of therapeutic immunosuppression. *Front Immunol*. 2018;9:275.
24. de Leur K, Dor FJ, Dieterich M, et al. IL-21 Receptor antagonist inhibits differentiation of B cells toward plasmablasts upon alloantigen stimulation. *Front Immunol*. 2017;8:306.
25. Dipchand AI, Webber S, Mason K, et al. Incidence, characterization, and impact of newly detected donor-specific anti-HLA antibody in the first year after pediatric heart transplantation:A report from the CTOTC-04 study. *Am J Transplant*. 2018;18:2163–2174.
26. Zhang Q, Hickey M, Drogalis-Kim D, et al. Understanding the correlation between DSA, complement activation and antibody mediated rejection in heart transplant recipients. *Transplantation*. 2018;102:e431–e438.
27. Zeevi A, Lunz J, Feingold B, et al. Persistent strong anti-HLA antibody at high titer is complement binding and associated with increased risk of antibody-mediated rejection in heart transplant recipients. *J Heart Lung Transplant*. 2013;32:98–105.
28. Leonardo SM, De Santis JL, Gehrand A, et al. Expansion of follicular helper T cells in the absence of Treg cells: implications for loss of B-cell anergy. *Eur J Immunol*. 2012;42:2597–2607.
29. Schmitt N, Liu Y, Bentebibel SE, et al. The cytokine TGF-beta co-opts signaling via STAT3-STAT4 to promote the differentiation of human TFH cells. *Nat Immunol*. 2014;15:856–865.
30. Noel C, Abramowicz D, Durand D, et al. Daclizumab versus antithymocyte globulin in high-immunological-risk renal transplant recipients. *J Am Soc Nephrol*. 2009;20:1385–1392.
31. Brennan DC, Daller JA, Lake KD, et al. Rabbit antithymocyte globulin versus basiliximab in renal transplantation. *N Engl J Med*. 2006;355:1967–1977.
32. Cherkassky L, Lanning M, Lalli PN, et al. Evaluation of alloreactivity in kidney transplant recipients treated with antithymocyte globulin versus IL-2 receptor blocker. *Am J Transplant*. 2011;11:1388–1396.
33. Louis S, Audrain M, Cantarovich D, et al. Long-term cell monitoring of kidney recipients after an antilymphocyte globulin induction with and without steroids. *Transplantation*. 2007;83:712–721.
34. O'Leary JG, Samaniego M, Barrio MC, et al. The influence of immunosuppressive agents on the risk of de novo donor-specific HLA antibody production in solid organ transplant recipients. *Transplantation*. 2016;100:39–53.
35. Brokhof MM, Sollinger HW, Hager DR, et al. Antithymocyte globulin is associated with a lower incidence of de novo donor-specific antibodies in moderately sensitized renal transplant recipients. *Transplantation*. 2014;97:612–617.
36. Wiebe C, Gibson IW, Blydt-Hansen TD, et al. Evolution and clinical pathologic correlations of de novo donor-specific HLA antibody post kidney transplant. *Am J Transplant*. 2012;12:1157–1167.
37. Krisl JC, Alloway RR, Shield AR, et al. Acute rejection clinically defined phenotypes correlate with long-term renal allograft survival. *Transplantation*. 2015;99:2167–2173.
38. Hricik DE, Formica RN, Nickerson P, et al. Adverse outcomes of tacrolimus withdrawal in immune-quiescent kidney transplant recipients. *J Am Soc Nephrol*. 2015;26:3114–3122.
39. de Graav GN, Dieterich M, Hesselink DA, et al. Follicular T helper cells and humoral reactivity in kidney transplant patients. *Clin Exp Immunol*. 2015;180:329–340.
40. Cano-Romero FL, Goya Laguna R, Utrero-Rico A, et al. Longitudinal profile of circulating T follicular helper lymphocytes parallels anti-HLA sensitization in renal transplant recipients. *Am J Transplant*. 2019;19:89–97.
41. Schmitt N, Bentebibel SE, Ueno H. Phenotype and functions of memory Tfh cells in human blood. *Trends Immunol*. 2014;35:436–442.
42. Schmitt N, Liu Y, Bentebibel SE, et al. Molecular mechanisms regulating T helper 1 versus T follicular helper cell differentiation in humans. *Cell Rep*. 2016;16:1082–1095.
43. Bouvy AP, Klepper M, Kho MM, et al. The impact of induction therapy on the homeostasis and function of regulatory T cells in kidney transplant patients. *Nephrol Dial Transplant*. 2014;29:1587–1597.

44. Wing JB, Ise W, Kurosaki T, et al. Regulatory T cells control antigen-specific expansion of Tfh cell number and humoral immune responses via the coreceptor CTLA-4. *Immunity*. 2014;41:1013–1025.
45. Korin YD, Lee C, Gjertson DW, et al. A novel flow assay for the detection of cytokine secreting alloreactive T cells: application to immune monitoring. *Hum Immunol*. 2005;66:1110–1124.
46. Heeger PS, Greenspan NS, Kuhlenschmidt S, et al. Pretransplant frequency of donor-specific, IFN-gamma-producing lymphocytes is a manifestation of immunologic memory and correlates with the risk of posttransplant rejection episodes. *J Immunol*. 1999;163:2267–2275.
47. Hricik DE, Rodriguez V, Riley J, et al. Enzyme linked immunosorbent spot (ELISPOT) assay for interferon-gamma independently predicts renal function in kidney transplant recipients. *Am J Transplant*. 2003;3:878–884.
48. Mulder A, Kardol MJ, Kamp J, et al. Determination of the frequency of HLA antibody secreting B-lymphocytes in alloantigen sensitized individuals. *Clin Exp Immunol*. 2001;124:9–15.
49. Zachary AA, Kopchaliiska D, Montgomery RA, et al. HLA-specific B cells: I. A method for their detection, quantification, and isolation using HLA tetramers. *Transplantation*. 2007;83:982–988.
50. Kim EJ, Kwun J, Gibby AC, et al. Costimulation blockade alters germinal center responses and prevents antibody-mediated rejection. *Am J Transplant*. 2014;14:59–69.
51. Badell IR, La Muraglia GM 2nd, Liu D, et al. Selective CD28 blockade results in superior inhibition of donor-specific T follicular helper cell and antibody responses relative to CTLA4-Ig. *Am J Transplant*. 2018;18:89–101.
52. Gensous N, Schmitt N, Richez C, et al. T follicular helper cells, interleukin-21 and systemic lupus erythematosus. *Rheumatology*. 2017;56:516–523.
53. Wu Y, van Besouw NM, Shi Y, et al. The biological effects of IL-21 signaling on B-cell-mediated responses in organ transplantation. *Front Immunol*. 2016;7:319.
54. Tchao NK, Turka LA. Lymphodepletion and homeostatic proliferation:implications for transplantation. *Am J Transplant*. 2012;12:1079–1090.